Spacetime structure of an inflating global monopole

Inyong Cho* and Alexander Vilenkin†
Tufts Institute of Cosmology, Department of Physics and Astronomy, Tufts University, Medford, Massachusetts 02155
(Received 5 August 1997)

The evolution of a global monopole with an inflating core is investigated. An analytic expression for the exterior metric at large distances from the core is obtained. The overall spacetime structure is studied numerically, both in vacuum and in a radiation background. [S0556-2821(97)02424-7]

PACS number(s): 98.80.Cq, 04.20.Gz, 14.80.Hv

I. INTRODUCTION

It has been argued in Refs. [1,2] that inflation can occur in the cores of topological defects. The condition for this is that the symmetry-breaking scale of the defects satisfy $\eta > \eta_c \sim \mathcal{O}(m_p)$. An attractive feature of this topological inflation is that it does not require fine-tuning of the initial conditions. The qualitative arguments of Refs. [1,2] were later verified in numerical simulations by Sakai *et al.* [3]. They found in particular that the critical value of η for domain walls and global monopoles is $\eta_c \simeq 0.33 m_p$.

In this paper, we would like to discuss the spacetime structure of inflating defects. This issue was partially addressed in Refs. [2,3]. However, some questions still remain unanswered. In particular, it is not clear what inflating defects look like from the outside. To be specific, consider the case of global monopoles. For $\eta < \eta_c$, the metric at large distances from the core has a solid deficit angle $\Delta \simeq 4\pi(8\pi G\eta^2)$ [4]. When $\eta > \eta_c$, the solid deficit angle exceeds 4π and static solutions do not exist. It was conjectured in Ref. [2] and verified in Ref. [3] that static solutions cease to exist at the same value of $\eta = \eta_c$ for which topological inflation becomes possible. The problem is then to determine the metric outside the inflating monopole. We shall address this problem both analytically and numerically.

In the next section, we review the static monopole solution of Ref. [4] and conjecture that the metric we are looking for is obtained by continuing this static metric to $\Delta > 4\pi$. This conjecture is then verified in Sec. III by numerically solving combined Einstein's and scalar field equations. (Here, we follow the technique of Sakai *et al.*) The overall spacetime structure of the inflating monopole is discussed in Sec. IV. In Sec. V, we study the global monopole dynamics with cosmological initial condtions which include a radiation background. Our conclusions are summarized in Sec. VI.

II. ASYMPTOTIC METRIC

The simplest model that gives rise to global monopoles is described by the Lagrangian

$$\mathcal{L} = -\frac{1}{2}\partial_\mu \phi^a \partial^\mu \phi^a - \frac{1}{4}\lambda(\phi^a\phi^a - \eta^2)^2, \tag{2.1}$$

where ϕ^a is a triplet of scalar fields, $a = 1,2,3$. The model has a global O(3) symmetry spontaneously broken down to U(1). A global monopole of unit topological charge is described by the ''hedgehog'' configuration $\phi^a = \phi(r)\hat{x}^a$, where $\hat{x}^a$ is a radial unit vector. Outside the monopole core, $\phi(r) \approx \eta$. By soving Einstein's equation in the asymptotic region outside the core, the metric is found to be [4]

$$ds^2 = -\left(1 - 8\pi G\eta^2 - \frac{2GM}{R}\right)dT^2 + \left(1 - 8\pi G\eta^2 - \frac{2GM}{R}\right)^{-1} dR^2 + R^2 d\Omega^2. \tag{2.2}$$

(We use $\hbar = c = 1, G = 1/m_p^2$.)

At large distances from the core, the mass term can be neglected, and after rescaling T and R coordinates the metric takes the form

$$ds^2 = -dT'^2 + dR'^2 + (1 - 8\pi G\eta^2)R'^2 d\Omega^2. \tag{2.3}$$

This metric exhibits a solid angle deficit $\Delta = 4\pi(8\pi G\eta^2)$. Another useful form of the global monopole metric can be obtained by a coordinate transformation

$$t = \frac{1}{\sqrt{|1-v^2|}}(T' - vR'), \quad r = \frac{1}{\sqrt{|1-v^2|}}(R' - vT'), \tag{2.4}$$

where $v = \sqrt{8\pi G\eta^2}$. This gives

$$ds^2 = -dt^2 + dr^2 + (r + \sqrt{8\pi G\eta^2}\,t)^2 d\Omega^2. \tag{2.5}$$

Let us now formally consider the metric (2.2) with a solid deficit angle $\Delta > 4\pi$. In this case, the asymptotic form of the metric is

$$ds^2 = -dR'^2 + dT'^2 + (8\pi G\eta^2 - 1)R'^2 d\Omega^2. \tag{2.6}$$

Here, T' is a spacelike and R' is a timelike coordinate. The natural ranges of these coordinates are $-\infty < T' < \infty$ and $0 < R' < \infty$. The metric (2.6) then represents a ''cylindrical'' universe of topology $R \times S(2)$. The expansion of this universe is highly anisotropic: There is no expansion in the T' direction along the axis of the cylinder, while the radius of the spherical sections grows proportionally to time (R').

The coordinate transformation (2.4) brings Eq. (2.6) to the form (2.5). Note that the metric (2.5) applies to both $\Delta < 4\pi$

*Electronic address: cho@cosmos2.phy.tufts.edu
†Electronic address: vilenkin@cosmos2.phy.tufts.edu

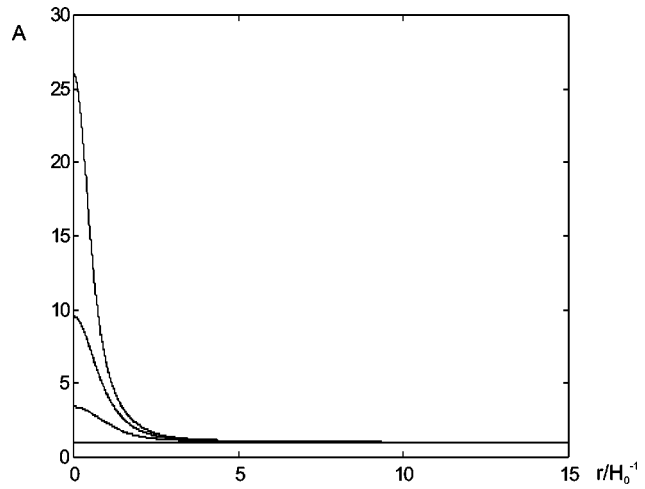

FIG. 1. A plot of $A(t,r)$ vs $H_0 r$ at $H_0 t = 1,2,3$ for $\eta = 0.6\, m_p$. Lower curves correspond to earlier times. At small r, $A(t,r)$ grows rapidly with time. In the asymptotic region, $A(t,r) \approx 1$.

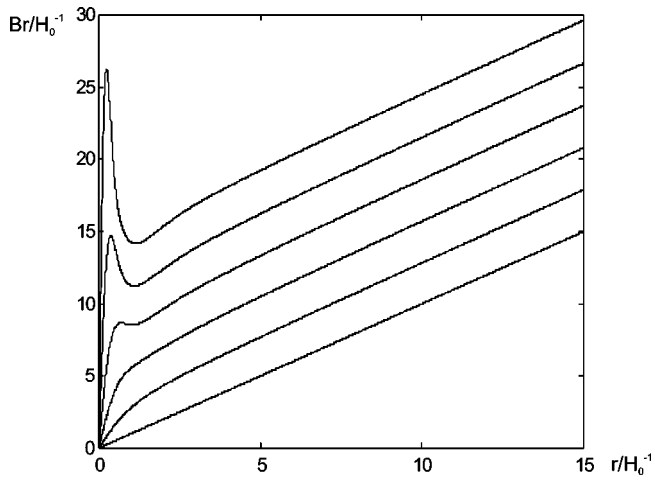

FIG. 2. A plot of $H_0 r B(t,r)$ vs $H_0 r$ at $H_0 t = 0,1,2,3,4,5$ for $\eta = 0.6\, m_p$. Lower curves correspond to earlier times. In the asymptotic region, lines are equally spaced and the separation is $\approx \sqrt{8\pi G \eta^2}$.

and $\Delta > 4\pi$. It is easily verified that Eq. (2.5) solves Einstein's equations with an energy-momentum tensor corresponding to the ansatz $\phi^a = \phi(r)\hat{x}^a$.

It seems reasonable to assume that Eqs. (2.5) and (2.6) represent the exterior asymptotic region of an inflating monopole. In the next section, we shall verify this assumption by numerically solving Einstein's and scalar field equations.

III. NUMERICAL RESULTS

In this section, we use the technique of Sakai *et al.* [3] to study the monopole evolution numerically. We use the general spherically symmetric ansatz for the metric

$$ds^2 = -dt^2 + A(t,r)^2 dr^2 + B(t,r)^2 r^2 d\Omega^2 \tag{3.1}$$

and the scalar field

$$\phi^a = \phi(t,r)\hat{x}^a. \tag{3.2}$$

The corresponding field equations are shown in the Appendix.

Following Sakai *et al.*, we set up the initial conditions by assuming the 3-metric to be flat at the initial moment, $t = 0$. The initial monopole field $\phi(0,r)$ is obtained by numerically solving the static flat-space field equation with the boundary conditions $\phi(r=0) = 0$ and $\phi(r=\infty) = \eta$. Finally, we set $\dot{\phi}(0,r) = 0$ and evaluate $\dot{A}(0,r)$ and $\dot{B}(0,r)$ from the Hamiltonian and the momentum constraints (A1) and (A2).

We solved the field equations with these initial conditions for several values of the symmetry-breaking scale η. Our results are in full agreement with those of Sakai *et al.* [3]. While the latter authors concentrated mainly on the inflating region in the monopole core, we shall analyze the asymptotic region and the overall structure of the monopole spacetime.

To illustrate our results, we shall take $\eta = 0.6\, m_p$, which is greater than the critical value $\eta_c = 0.33\, m_p$. The solutions $A(t,r)$ and $B(t,r)r$ are shown as functions of r at several moments of time in Figs. 1 and 2, respectively. In the figures, r and t are shown in units of $H_0^{-1} = [8\pi G V(\phi = 0)/3]^{-1/2}$, which is the horizon radius at the monopole center. At small r we clearly have inflation: Both A and B rapidly grow with time, with $A \approx B$.

Now, it is easily verified that for $r \gtrsim 4H_0^{-1}$ the metric is well approximated by Eq. (2.5): Figure 1 shows that $A(t,r) \approx 1$, and Fig. 2 shows that the graphs of $B(t,r)r$ at $H_0 t = 0,1,2,3,4,5$ are equally spaced straight lines. The quantitative agreement with the coefficient $\sqrt{8\pi G \eta^2}$ in Eq. (2.5) is also easily checked.

IV. SPACETIME STRUCTURE

The overall spacetime structure of an inflating monopole is illustrated in an r-t diagram in Fig. 3. The inflating region of spacetime is the region where the slow-roll condition is satisfied,

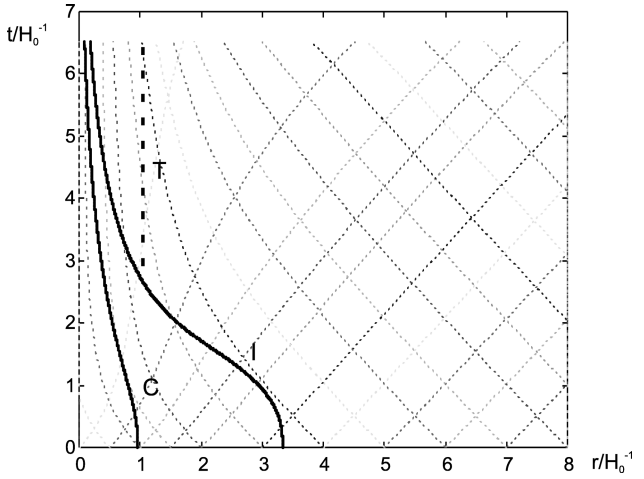

FIG. 3. r-t diagram illustrating the spacetime structure of an inflating monopole of $\eta = 0.6\, m_p$. The light dotted lines are ingoing and outgoing null geodesics. The line I is the boundary of the inflating region and the line C is the boundary of the monopole core where $\phi(t,r) = \eta/2$. These two lines, I and C, represent spacelike hypersurfaces. The heavy dotted line T is the location of the throat.

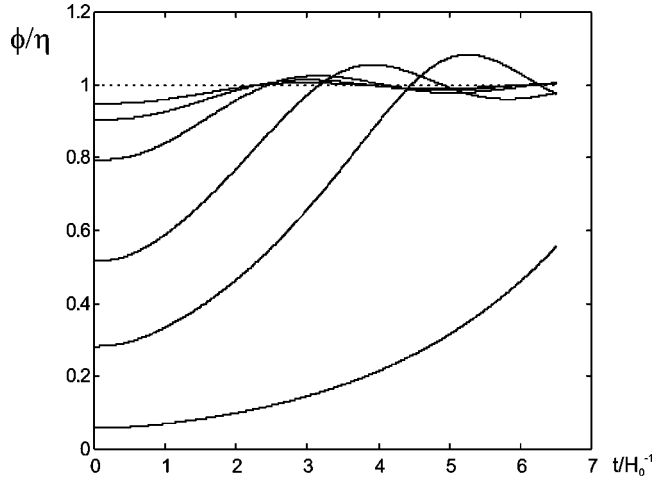

FIG. 4. Evolution of the scalar field at a fixed r, for $H_0 r = 0.1,0.5,1,2,3,4$ from the bottom. The scalar field at small r spends much time near the top of the potential while it undergoes inflation. The field at large r comes out of the inflating region earlier and oscillates about its vacuum expectation value η.

$$V'(\phi) \ll (48\pi G)^{1/2} V(\phi). \tag{4.1}$$

The boundary of this region is shown by line I in the diagram. Also shown is the boundary of the monopole core, which is defined as the region inside the surface $\phi(t,r) = \eta/2$ (line C). Both surfaces are spacelike (as all surfaces of constant ϕ in the slow-roll region).

Let us consider the evolution of the metric and the scalar field along a timelike geodesic $r = \text{const}$ (the geodesic is not shown in the figure). In Fig. 4, the field ϕ is shown as a function of t for several values of r. We first choose $r < H_0^{-1}$, so that the comoving observer, whose trajectory this geodesic represents, starts inside the core at $t = 0$. As the field ϕ rolls down the slope of the potential, the observer will come out of the core region and later out of the inflating region. At this point ϕ will start to oscillate about its vacuum expectation value η. (This oscillation is clearly visible in Fig. 4.) The effective equation of state for such an oscillating field, averaged over the period of oscillation, is that of a pressureless dust. Hence, our observer emerges from an inflating to a matter-dominated region. In a more realistic model, the oscillations of ϕ would be damped by particle production, resulting in a hot thermal radiation, but this does not happen in our simple model.

Observers with a comoving coordinate r between H_0^{-1} and $3H_0^{-1}$ start outside the monopole core, but otherwise follow the same evolution and end up in a matter-dominated region. On the other hand, observers with $r > 4H_0^{-1}$ have their starting points outside the inflating region, and their surroundings are well described by the asymptotic exterior metric (2.5).

Since the boundary of the inflating region is spacelike, no observer can get into that region from the exterior or matter-dominated regions. This can be seen by examinimg the null geodesics, shown by dotted lines in Fig. 3.

To illustrate the geometry of equal-time surfaces, $t = \text{const}$, in the monopole spacetime, we shall use a lower-dimensional version of the metric (3.1) with one of the angular dimensions suppressed. The 2-metric is then

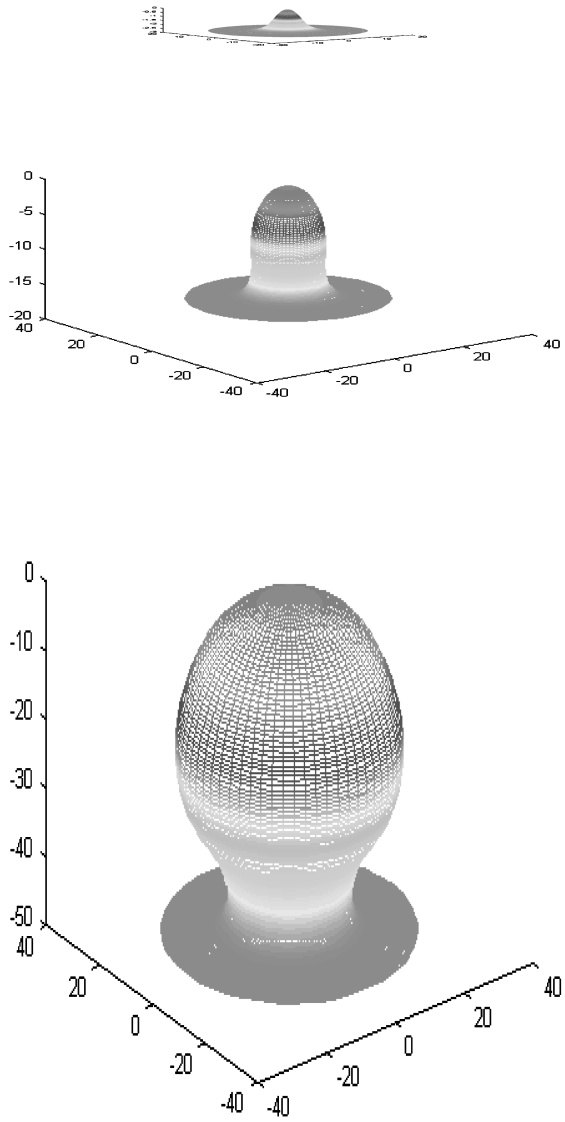

FIG. 5. A 2D slice of the inflating monopole ($\eta = 0.6\, m_p$) geometry embedded in a 3D Euclidean space at $H_0 t = 1,3,5$ (from the top down). The space gets curved around the monopole core and an inflating balloon is formed later while the asymptotic region remains flat. A throat is developed between these two regions.

$$ds^2 = A(t,r)^2 dr^2 + B(t,r)^2 r^2 d\theta^2. \tag{4.2}$$

Embeddings of this metric in a 3-dimensional (3D) Euclidean space [5] are shown in Fig. 5 for several moments of time. We see that the spatial geometry is that of an inflating balloon connected by a throat to an asymptotically flat region at large r. The throat is developed soon after the onset of inflation. Figure 5 is similar to the figure in Sakai *et al.* [3], which shows a 3D graph of proper radius $rB(t,r)$ vs proper length $\int A(t,r)dr$ (rather than the embedded 2-geometry).

The location of the throat, determined from $d(Br)/dr = 0$, is indicated by line T in Fig. 3. It is well approximated by a constant-r line, $r \simeq H_0^{-1}$.

V. MONOPOLE EVOLUTION WITH COSMOLOGICAL INITIAL CONDITIONS

So far, we considered global monopoles coupled only to gravitation. But cosmologically, monopoles are formed at a

phase transition, and the monopole energy is taken from the energy of thermal radiation. In this section we shall consider the evolution of a global monopole in a radiation background.

We use the same metric and scalar field ansatz as in Sec. III. The energy-momentum tensor of monopole-plus-radiation system is

$$T^{(\mathrm{tot})}_{\mu\nu}=T^{(m)}_{\mu\nu}+T^{(r)}_{\mu\nu}. \tag{5.1}$$

The energy-momentum tensor of radiation is that of a perfect fluid with an equation of state $P=\frac{1}{3}\rho$,

$$T^{(r)}_{\mu\nu}=(\rho+P)u_\mu u_\nu+Pg_{\mu\nu}=\frac{\rho}{3}(4u_\mu u_\nu+g_{\mu\nu}), \tag{5.2}$$

where u^μ is the velocity 4-vector,

$$u^\mu=\left(\frac{1}{\sqrt{1-v^2}},\frac{v}{A\sqrt{1-v^2}},0,0\right).$$

Prior to the phase transition, the space is filled with isotropic radiation fluid, and so the metric is that of Friedman-Robertson-Walker (FRW) in the radiation-dominated era, and

$$\rho^{(r)}(t)=\frac{3}{32\pi G t^2}. \tag{5.3}$$

A realistic initial condition at the time of monopole formation, t_0, is $\rho^{(\mathrm{tot})}(t_0,r)=\rho^{(m)}(t_0,r)+\rho^{(r)}(t_0,r)=\mathrm{const}$, with $\rho^{(m)}\sim\rho^{(r)}$ near the monopole core. For computational purposes, it is better to use a somewhat different initial condition

$$\rho^{(r)}(t_0,r)=\mathrm{const}. \tag{5.4}$$

We tried them both and found the results to be very similar. The initial condition (5.4) is preferable because it allows us to choose the initial value of $\rho^{(r)}$ somewhat lower than the core energy density $V(0)$ and run the evolution until a later cosmic time. (We stop the run when numerical instabilities develop in the inflating core region.)

The results presented below in this section were obtained using the following initial conditions: $A(t_0,r)=B(t_0,r)=1$, $v(t_0,r)=0$, $\phi(t_0,r)$ the same as in the vacuum case, $\dot\phi(t_0,r)=0$ and $\rho^{(r)}(t_0,r)=0.1\,V(0)$. The moment t_0 is determined by the initial value of $\rho^{(r)}$ from Eq. (5.3).

The field equations for the monopole-plus-radiation system, with a brief outline of the method of their solutions, are given in the Appendix. Not surprisingly, we found that the critical symmetry-breaking scale η_c is the same as in the vacuum case, $\eta_c\approx 0.33\,m_p$. Our results for $\eta=0.6\,m_p$ are presented in Figs. 6–8.

Figure 6 shows that $B/A\approx 1$ in the inflating core and in the asymptotic region. We have checked that the region of large r exhibits the usual radiation-dominated evolution,

$$A\approx B\approx(t/t_0)^{1/2}. \tag{5.5}$$

In this region, the energy density of the monopole falls off as

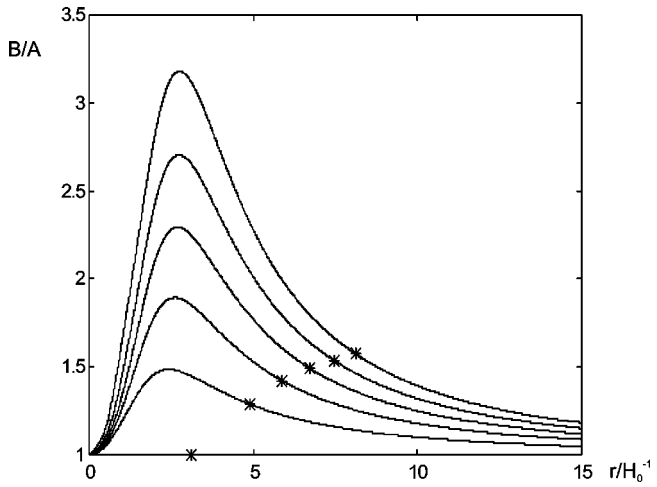

FIG. 6. A plot of $B(t,r)/A(t,r)$ vs H_0r at $H_0(t-t_0)=0,1,2,3,4,5$ for a monopole of $\eta=0.6\,m_p$ with the initial radiation density $\rho^{(r)}(t_0,r)=0.1\,V(0)$. Lower curves correspond to earlier times. It shows that $A(t,r)\approx B(t,r)$ at small and large r. The positions where $\rho^{(m)}=\rho^{(r)}$ are indicated by an asterisk.

$$\rho^{(m)}\sim\frac{\eta^2}{B(t,r)^2r^2}\sim\frac{\eta^2}{(t/t_0)r^2}.$$

On the other hand, the radiation density is approximately homogeneous, but it damps more rapidly with time as in Eq. (5.3). The two densities are comparable at

$$r\approx(32\pi G\eta^2t_0/3)^{1/2}\sqrt{t}\approx 1.9\,(\eta/\eta_c)\sqrt{t_0t}. \tag{5.6}$$

We can expect the region outside this surface to be well approximated by a FRW radiation-dominated universe, and the interior region to have spacetime structure similar to that of the vacuum solution discussed in the preceding section.

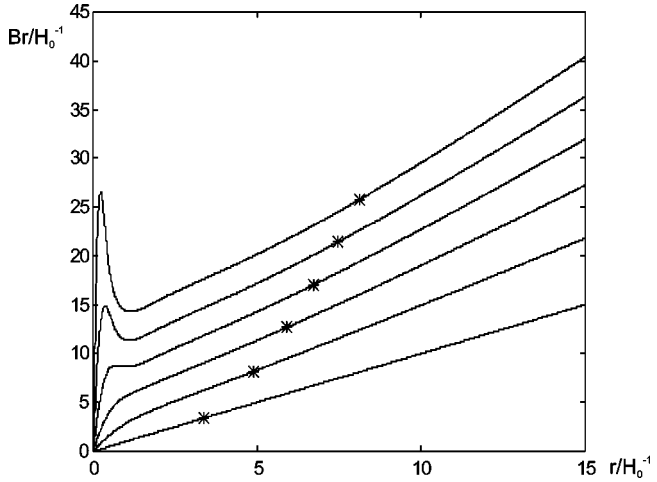

FIG. 7. A plot of $H_0rB(t,r)$ vs H_0r at $H_0(t-t_0)=0,1,2,3,4,5$ for a monopole of $\eta=0.6\,m_p$ with the initial radiation density $\rho^{(r)}(t_0,r)=0.1\,V(0)$. Lower curves correspond to earlier times. To the left of the asterisks, the plot is similar to that of the vacuum solution in Fig. 2. The positions where $\rho^{(m)}=\rho^{(r)}$ are indicated by an asterisk.

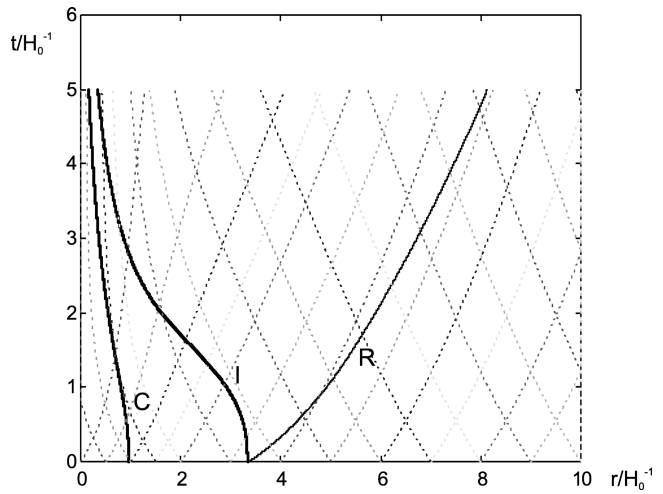

FIG. 8. r-t diagram illustrating the spacetime structure of an inflating monopole of $\eta=0.6\,m_p$ in a radiation background with $\rho^{(r)}(t_0,r)=0.1\,V(0)$. The line I is the boundary of the inflating region and the line C is the boundary of the monopole core where $\phi(t,r)=\eta/2$. The line R is the boundary where $\rho^{(m)}=\rho^{(r)}$.

These expectations are supported by our numerical results: We see a structure very similar to Fig. 2 emerging on the left-hand side of Fig. 7.

The overall spacetime structure is shown in Fig. 8, where the surface $\rho^{(m)}=\rho^{(r)}$ is indicated by the line R. This line is reasonably well approximated by Eq. (5.6). (The fact that the line R coincides with the boundary of the inflating region I at $t=t_0$ is a numerical coincidence.)

Comparing Eq. (5.6) with the null geodesic in metric (5.5), $r=2\sqrt{t_0 t}$, we see that the boundary (5.6) expands faster than the speed of light (unless perhaps when η is very close to η_c). Hence, physical observers cannot get from the exterior vacuum region (dominated by the scalar field) to the radiation-dominated region.

VI. CONCLUSIONS

We have investigated the spacetime structure of an inflating global monopole, both inside and outside the inflating core. We found that the inflating region near the core is surrounded by a ''matter'' region, where the dominant contribution to the energy is that of an oscillating scalar field. The inflating region and most of the matter region are contained in an expanding ''balloon'' which is connected by a throat to the exterior region.

The exterior metric at large distances from the throat is well approximated by Eq. (2.5). This metric is obtained by analytic continuation of the static monopole metric (2.2), followed by a coordinate transformation (2.4). It describes a nonstationary spacetime with a highly anisotropic expansion.

A spaceship from the exterior region can pass through the throat and get into the matter-dominated region, but it cannot get into the inflating region. The inflating region is bounded by a spacelike hypersurface and is seen by observers in the matter region as an epoch in their past.

To simulate the formation of an inflating monopole at a cosmological phase transition, we studied the monopole evolution in a radiation background. At the initial moment, the radiation energy dominates everywhere, except in the central region near the core. However, this energy is redshifted faster than that of the scalar field, and as a result the boundary of the radiation-dominated region is pushed to larger and larger distances. The spacetime structure emerging at large t inside this boundary is very similar to that in the vacuum case without radiation.

It would be interesting to perform a similar analysis for topological defects other than global monopoles. In the case of gauge monopoles, we expect [2] the exterior region to be described by the Reissner-Nordström metric. For strings and domain walls, the situation is not so clear. This problem is now being investigated.

ACKNOWLEDGMENTS

We are grateful to Nobuyuki Sakai for helpful correspondence and to the National Science Foundation for partial support.

APPENDIX: FIELD EQUATIONS FOR THE MONOPOLE-RADIATION SYSTEM

Einstein's equations with the metric (3.1) and energy-momentum tensor (5.1) are

$$-G_0^0=K_2^2(2K-3K_2^2)-2\frac{B''}{A^2B}-\frac{B'^2}{A^2B^2}+2\frac{A'B'}{A^3B}-6\frac{B'}{A^2Br}+2\frac{A'}{A^3r}-\frac{1}{A^2r^2}+\frac{1}{B^2r^2}$$
$$=8\pi G\left[\frac{\dot\phi^2}{2}+\frac{\phi'^2}{2A^2}+\frac{\phi^2}{B^2r^2}+\frac{\lambda}{4}(\phi^2-\eta^2)^2+\frac{1}{3}\left(\frac{4}{1-v^2}-1\right)\rho\right], \tag{A1}$$

$$\frac{1}{2}G_{01}=K_2^{2\prime}+\left(\frac{B'}{B}+\frac{1}{r}\right)(3K_2^2-K)=4\pi G\left(\dot\phi\phi'-\frac{4}{3}\frac{v}{1-v^2}A\rho\right), \tag{A2}$$

$$\frac{1}{2}(G_1^1+G_2^2+G_3^3-G_0^0)=\dot K-(K_1^1)^2-2(K_2^2)^2=8\pi G\left[\dot\phi^2-\frac{\lambda}{4}(\phi^2-\eta^2)^2+\frac{1}{3}\left(1+2\frac{1+v^2}{1-v^2}\right)\rho\right], \tag{A3}$$

where

$$K_1^1=-\frac{\dot A}{A},\quad K_2^2=K_3^3=-\frac{\dot B}{B},\quad K=K_i^i. \tag{A4}$$

The conservation of the energy-momentum tensor, $T_{;\nu}^{(r)\mu\nu}=0$, gives two equations for ρ and v:

$$(3-v^2)\dot{v} = -\frac{2v}{A}v' - \frac{3(1-v^2)^2}{4A}\frac{\rho'}{\rho} + 2(K_1^1 - K_2^2)v(1-v^2) + 2\left(\frac{B'}{B} + \frac{1}{r}\right)\frac{v^2(1-v^2)}{A}, \tag{A5}$$

$$\frac{\dot{\rho}}{\rho} = \frac{8v}{3(1-v^2)^2}\dot{v} - \frac{4(1-3v^2)}{3A(1-v^2)^2}v' + K_1^1\frac{4(1-3v^2)}{3(1-v^2)} + K_2^2\frac{8}{3(1-v^2)} - \left(\frac{B'}{B} + \frac{1}{r}\right)\frac{8v}{3A(1-v^2)}. \tag{A6}$$

The field equation for ϕ is

$$\ddot{\phi} - K\dot{\phi} - \frac{\phi''}{A^2} - \left(-\frac{A'}{A} + \frac{2B'}{B} + \frac{2}{r}\right)\frac{\phi'}{A^2} + \frac{2\phi}{B^2r^2} + \frac{dV}{d\phi} = 0. \tag{A7}$$

With the initial conditions given in Sec. V, $K(t_0,r)$ and $K_2^2(t_0,r)$ are evaluated by the Hamiltonian and the momentum constraint equations (A1) and (A2). In the next time step, $v(t,r)$ and $\rho(t,r)$ are calculated by Eqs. (A5) and (A6). $A(t,r)$ and $B(t,r)$ are calculated by Eq. (A4), $\phi(t,r)$ by the scalar field equation (A7), and K_2^2 and K by the constraint equations (A2) and (A3). We apply the regularity condition $K_1^1(t,r=0) = K_2^2(t,r=0)$ at the origin.

The field equations in the vacuum case are obtained by setting $\rho = 0$ in Eqs. (A1)–(A3).

[1] A. D. Linde, Phys. Lett. B **327**, 208 (1994).
[2] A. Vilenkin, Phys. Rev. Lett. **72**, 3137 (1994).
[3] N. Sakai, H. Shinkai, T. Tachizawa, and K. Maeda, Phys. Rev. D **53**, 655 (1996); N. Sakai, *ibid.* **54**, 1548 (1996).
[4] M. Barriola and A. Vilenkin, Phys. Rev. Lett. **63**, 341 (1989).

[5] The metric of a 3D Euclidean space is $ds^2 = dz^2 + d\rho^2 + \rho^2 d\theta^2$. Comparing this with Eq. (4.2), we have $\rho = Br$ and $z' = \pm[A^2 - (B'r + B)^2]^{1/2}$, where the primes indicate derivatives with respect to r. The embedding is specified by the functions $\rho(r)$ and $z(r)$ which can be found from the above equations. The vertical axis in Fig. 5 is the z axis.